Research Article

Open Access

Journal of Herbal Medicine and Medicinal Plants

JHMP@scientificeminencegroup.com

Synthesis of Cerium Oxide Nanoparticles using Citrus Paradisi Peel Aqueous Extract and their Effect on Protein Aggregation, and Acetylcholinesterase Inhibition

Rosa Martha Perez Gutierrez[1,*], Angelica Celeste Torres Rivera[1], Fernando Martinez Jeronimo[2], Julio Tellez Gomez[1] and Jesus Carlos Sanchez Ochoa[1]

[1]Research Laboratory of Natural Products, School of Chemical Engineering and Extractive Industries-National Polytechnic Institute, Av. Instituto Politecnico Nacional S/N, Col. Zacatenco, Unidad Profesional Adolfo Lopez Mateos, 07758, Ciudad de Mexico, CP, Mexico

[2]Experimental Hydrobiology Research Laboratory, National School of Sciences, Biological National Polytechnic Institute (IPN)

*Corresponding Author

Rosa Martha Perez Gutierrez, Research Laboratory of Natural Products, School of Chemical Engineering and Extractive Industries-National Polytechnic Institute, Av. Instituto Politecnico Nacional S/N, Col. Zacatenco, Unidad Profesional Adolfo Lopez Mateos, 07758, Ciudad de Mexico, CP, Mexico, E-mail: rmpg@prodigy.net.mx

Citation

Rosa Martha Perez Gutierrez, Angelica Celeste Torres Rivera, Fernando Martinez Jeronimo, Julio Tellez Gomez, Jesus Carlos Sanchez Ochoa (2024) Synthesis of Cerium Oxide Nanoparticles using Citrus Paradisi Peel Aqueous Extract and their Effect on Protein Aggregation, and Acetylcholinesterase Inhibition. J Herb Med Plants 2: 1-19

Publication Dates

Received date: January 28, 2024

Accepted date: February 28, 2024

Published date: March 02, 2024

Abstract

Introduction: Acetylcholinesterase and protein aggregation are two important parameters contribute to the initiation and progression of the Alzheimer's disease. The aim of this study was to evaluate the association between CeO2NPs and flavonoids from grapefruit peel extract (To) to investigate their effect on protein aggregation and acetylcholinesterase inhibition in vitro.

Methods: Nanoparticles were obtained using stabilize and a sol-gel method was used, characterized using by Fourier transform infrared spectroscopy (FTIR), ultraviolet spectroscopy (UV-Vis), dynamic light scattering (DLS), transmission electron microscopy (TEM), zeta potential and x-ray powder diffraction (XRD). The effect of To/CeO2 NPs on aggregation protein was detected by Congo red, thioflavin T test, and fluorescence, dynamic light scattering (DLS), thermal aggregation, and turbidity assay in BSA-glucose system at 30 day of incubation. Acetylcholinesterase (AChE) inhibition activity was measured via a colorimetric assay. . The viability was evaluated on normal RAW 264.7 macrophage cell.

Results: The nanoparticles had a negative zeta potential of -22.6 mV indicating the great stability of the colloid in the aqueous medium, with average size of 199 nm, and

polydispersity index of 0.460 demonstrating homogenous size population. The TEM images of To/CeO2 NPs indicated a spherical shape and moderately agglomerated. Thus, the UV spectra of To/CeO2 NPs, XRD analysis and FTIR analysis supported that that To was successfully absorbed on the surface of nanoparticles. To/CeO_2 NPs inhibit fibril formation, protein aggregation, protect structural modifications in BSA-glucose system, inhibit AChE. Exposure to nanoparticles does not produce any substantial negative effect on RAW 264.7 viability cell .

Conclusions: To/CeO2 NPs displayed better neuroprotective effects than donepezil, uses as positive control, could be useful in the development of therapeutic new based in nanomedicine with a potential to be transferred into the clinic for the treatment of neurodegenerative diseases.

Keywords: Citrus Paradisi; Cerium Oxide Nanoparticles; Alzheimer's disease; Amyloid; Acetylcholinesterase

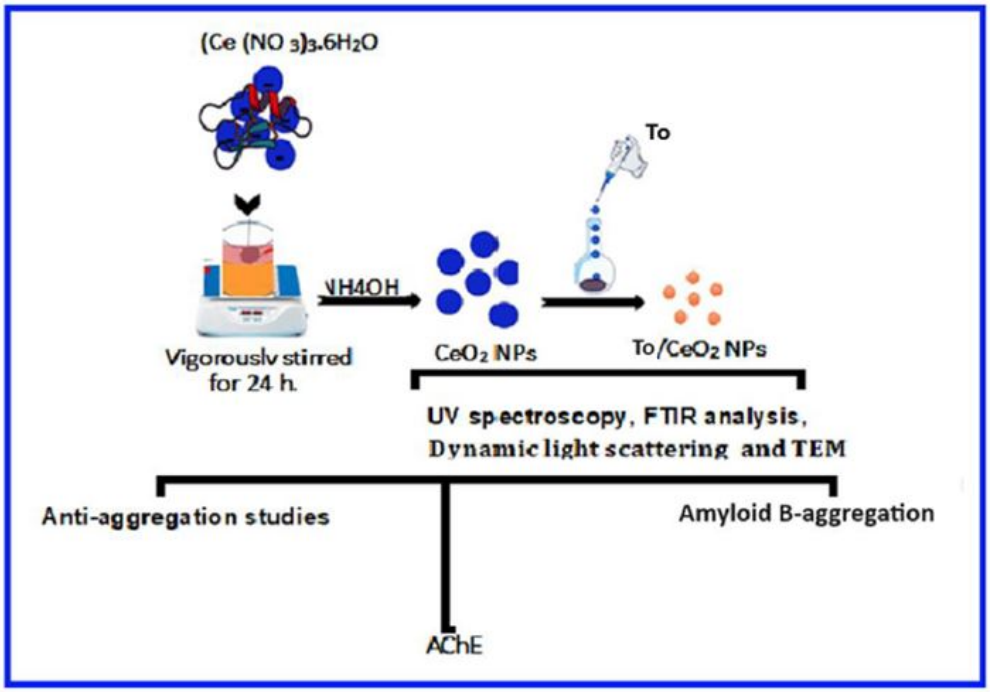

Graphical Abstract

Introduction

The unfavorable consequence of protein aggregation on safety and health in humans can be associated with multiple factors and have been related with the aging process, amyloid diseases, neurodegenerative diseases and enhanced cytotoxicity [1].The aggregating proteins in the form of neurofibrillary tangles contribute to neurotoxicity in Alzheimer's disease (AD) which be composed by extracellular senile plaques, and hyperphosphorylated tau 1,2 deposited in small peptides of amyloid-β (Aβ) derived from sequential proteolytic cleavages of the amyloid precursor protein (APP) 3 [2]. These mutations produce a deep change APP metabolism, facilitating the generation of aggregation-prone Aβ species, in this context, "amyloid cascade hypothesis" form the basis for the of AD pathogenesis [3].

Numerous studies have suggested that the learning and memory deficits related with aging and AD are ascribable to deterioration of the cholinergic magnocellular neurons of the nucleus basalis of Meynert (nbM). Degeneration of neural pathways imply transmitters as well as serotonin, acetylcholine, dopamine and noradrenaline [4]. In addition, a significant reduction in cholinergic markers and choline acetyltransferase, have been identified in demented patients [5]. In accordance with to this hypothesis, the changes in memory and learning deficits occurred in the AD and could be associated to a deterioration of the cholinergic systems of the basal forebrain [6,7].

Acetylcholinesterase (AChE) is a cholinergic enzyme hydrolyzes acetylcholine (ACh) or is breaks down into choline and acetic acid, an AChE over-expression increase congregation of Aβ into the amyloid fibrils that produce the senile plaques

characteristic of AD [8]. Thus, a reduction in Ach produce deficit in cholinergic neurotransmission [9].

Citric fruits and their chemical content as well as flavonoids and essential oil (terpenes) have effect on several diseases of the central nervous system, such as Parkinson's and Alzheimer's disease. The *C. paradisi* essential oil has shown Inhibition of acetylcholinesterase activity [10], their infusions from peel exhibited inhibition of monoamine oxidase and butyrylcholinesterase activities [11]. *C. paradisi* has a strong anxiolytic activity in elevated plus-maze [12].

The produced flavonoids compounds by plants are very abundant in fruits, and vegetables all of them are present in the human diet [13].Flavonoids can be found in all parts of plants because they are biosynthesized as defense against different kinds of stress such as cold tolerance. Flavonoids are derived from phenol, are known for their ability to cross the blood–brain barrier and for their numerous target effects. Flavonoids have important biologic effects involving antiamyloidogenic activities, the neuronal antioxidants; enhance neuroprotection and cognition, anti-inflammatory effects, metal chelators properties among others [14]. A diet rich in flavonoids helps to safeguard the efficiency and the number of neurons as well as their synaptic connections reducing the appearance of dementia and improving symptomatology in patients with neurodegenerative diseases [15].

The mechanism of action of the flavonoids in Alzheimer's disease involves the inhibition of butyrylcholinesterase, acetylcholinesterase, inflammation, apoptosis, oxidative stress, Tau protein aggregation, and β-secretase, through modulation of signaling pathways involve in neuroprotective and cognitive functions, such as MAPKs, NFKB, PI3-kinase/Akt, and ERK, and antioxidant enzymatic systems [16].

Citrus fruits contain great amounts of flavanones, as well as narirutin, hesperidin, naringin and polymethoxylated flavones like tangeretin, and nobiletin. The content of these flavonoids varies between citrus varieties. Several studies have demonstrated that citrus flavonoids are less abundant in the edible parts than in the pericarp [17]. High concentrations of flavonoids such as Lucenin-2, Vicenin-2, 3 Narirutin 4' -O-glucoside, Neoeriocitrin, Rutin, Narirutin, Hesperidin, Neoponcirin, Sinensetin, Nobiletin and Tangeretin [18]. Cigranoside C, Isoquercitrin, Naringin, Cigranoside E, Bergamjuicin, Rhoifolin, Neohesperidin, Cigranoside, Cigranoside B, Melitidin, and Cigranoside D have been found in *C. paradisi*, peel [19]. The combination of plant bioactive with biologic r effects increase the overall activityas a result of synergism [20] as consequence of stabilize the other drug in the system and increase the bioavailability of the drug.

Ultrasonic extraction methodology is a new technique for extract bioactive ingredients from plants b into solvents y using cavitation, strong vibration, and comminution produced by ultrasonic. The technique is very efficient, simple, and less by-products, and produces better results than the standard extraction. The generated by-products in ultrasonic extraction of the flavonoids include polysaccharide, protein, starch, compounds, together with flavonoids derivatives [21].

Nano medicine is associated with nanoparticles used for diagnostic and therapeutic purposes. A recent number of nano medicines displayed promise for future clinical transfer having received regulatory approval. It is vitally important that the safety measure test could be modified to be more suitable for engineered nanoparticles. Considering that the nanoparticles are manufactured with different materials have various type of risks related with them. The use of nanotechnologies can increase the bioavailability and/or solubility of bioactive and provide potential advantage in different therapies, involving selective targeting. Cerium oxide nanoparticles (CeO_2 NPs) have recently been considered for biomedical applications by their potent antioxidant, auto-regenerative properties, low toxicity, safety, tolerability, and bioavailability good .The considerable number of preclinical studies of CeO_2 NPs on retinal degenerations treatment, could pave the way to the clinical studies in humans for preventing retinal degeneration, cataracts, and other ocular diseases [22]. Dex-CeO_2 nanoparticles produced strong CT contrast (is an X-ray-based medical imaging test that can produce free-radical generation, possibility with adverse effects) in the GIT and accumulated in intestine affected by colitis by 24 h then administration. Thus, Dex-Ce O2NP has potential as a CT contrast agent for GIT imaging as well as imaging IBD [23]. Preclinical studies indicated a good potential for clinical transfer attributable to advantageous clearance profile. The application in soft tissue engineering of the 3D printing procedure could be convenient to suitably design the structure of the implants in which Ce O2NPsare incorporated in the attempt to bind the nanoparticles release for carried out the best therapeutic effects [24].

The biological activity of phenolic compounds is due to different functional groups, which show diverse forms of interaction forces. Thus, related the limitation to the structure is its poor bioavailability and low solubility. These deficiencies can be overcome by the use of nanoparticles delivery systems, have which shown an increase in bioavailability, stability and high-water solubility [25]. The citrus flavonoids after oral administration remaining unabsorbed in the colon limiting its bioavailability [25] favoring the application of nanoparticles.

The purpose of this investigation to describe the synthesis and characterization of Cerium oxide nanoparticles functionalized with C. paradisi peel aqueous extract (To/CeO2 NPs) as well as to highlight from its potential protective on protein aggregation and acetylcholinesterase inhibition with the goal of finding as potential treatment of Alzheimer's disease. The advantage of To/CeO2 NPs is the possibility of adding them to food supplements.

Materials and Methods

Chemicals and Plant Material

The metal precursor cerous nitrate and the other chemicals required for the preparation of anoparticles were purchased from Sigma (St. Louis, Mo, USA). The fruits of the Lemon [*Citrus x paradisi*] were obtained from commercial source and confirmed in the herbarium of the National School of Biological Sciences México (78957).

Preparation of Peel Extract

The *C. paradisi* peels were washed with bidistilled water and then cut into small fragments. 350 g of fruit peels were mixed with 900 mL of Milli-Q water, the extraction was performed with an Ultrasound-assisted extraction (Cole-Parmer, Vernon Hills, IL, USA). The pulse mode with 2 s ON and 2 s OFF. The extraction time was of 30 min using a temperature of 45 ◦C and working frequency was fixed at 40 kHz. The obtained extract was then filtered through a filter No 42 Whatman.

Determination of Total Flavonoids

The total flavonoids content in to peels was determined by a colorimetric test. 10 mL of the extract was mixed with NaNO2 solution (5%; 0.3 ml). The mixture was left to stand for 6 min at room temperature; then Al(NO3)3 solution (5% ; 0.3 ml) was added to the mixture which was kept for other 6 min at room temperature. Finally, NaOH solution (4%; 4.4 ml) was added was left to rest for 12 min at room temperature. The UV-visible spectra were obtained using an 1810 UV-spectrophotometer (Beijing, China) at 510 nm, and the flavonoids percentages were estimated using calibration curves.

Synthesis of CeO2 NPs

A method sol-gel was used for the synthesis of CeO2 nanoparticles using the sol-gel method, 6.3 g of cerium nitrate hexahydrate (Ce (NO 3)3.6H2O, (Sigma, St. Louis, Mo, USA) was dissolved in 300 ml of Milli-Q water and the mixture was stirred for 30 min. 10% NH4OH was added drop a drop maintaining a pH between 7-8, then the mixture was vigorously stirred room temperature for 24 h. The solution was centrifuged at 20,00 rpm for 30 min to remove the excess cerium nitrate and other precursors. The supernatant was discarded, and the obtained pellet was washed with Milli-Q water. The solution containing CeO2 NPs was dialyzed against Milli-Q water for 24 h and stored at room temperature. Initially, the reaction mixture turned into a light-yellow color, and then the appearance of an intense yellow color confirmed the presence s of CeO2NPs.

Synthesis of To/CeO2 NPs

0.4 g of cerium nanoparticles was mixed with 0.2 g of *C. paradisi* extract and vigorously stirred continuously at room temperature for 6 h. The solution was centrifuged at 20,00 rpm for 30 min. The supernatant was discarded, and the pellet was washed with Milli-Q water. The solution containing To/CeO2 nanoparticles was dialyzed against Milli-Q water for 24 h and stored at room temperature.

Characterization of CeO2 and to/CeO2NPs

The size and polydispersity of the CeO2NPs were analyzed by dynamic light scattering (DLS). Zeta potential of CeO2NPs and To/CeO2 NPs was measured using a Zetasizer Nano ZSP (Malvern Instruments, Malvern, UK.) Both measures were made by triplicate at 25 °C. The surface morphology of cerium nanoparticles was analyzed using a high-resolution transmission electron microscope (TEM; Model HT7700, Hitachi High-Tech, Tokyo, Japan). Infrared spectrum of nanoparticles was obtained with a spectrophotometer FTIR-TENSOR27, Bruker, Ettinger, Germany, in the range of 400–4000

cm^{-1}. The UVvisible spectra were obtained using a UV-1800 Shimadzu spectrophotometer in Tokyo, Japan. X-ray photoelectron spectroscopy (XPS) was performed using a spectrometer with a monochromatic Al Kα xray source (Thermo-Fisher ESCALAB 250xi).

Encapsulation Efficiency (EE, %) and Loading Capacity (LC, %) of To in CeO2 NPs

To-loaded CeO2 NPs was carried out according to the earliest investigation. Briefly, To -loaded CeO2 NPs (30 mg) were dispersed into MeOH and stirred at 600 rpm for 3 h. Then, the mixture was centrifugated at 10000 × g for 1 h [26]. Supernatant was collected and the content of unencapsulated extract was calculated from a calibration curve using a UV-1800 spectrophotometer (Shimadzu Corporation, Kyoto, Japan) at 257.5 nm. The EE, % and LC, % of To extract was determined by using the following equations [27].

$$Encapsulation\ efficiency\ EE\ (\%) = \frac{Amount\ of\ encapsulated\ To\ extract}{Total\ amount\ of\ To\ extract} \times 100 \quad (1)$$

$$Loading\ capacity\ (LC\%) = \frac{Amount\ total\ To\ extract\ entrapped}{The\ total\ Cerium\ NPs\ weight} \times 100 \quad (2)$$

Acetylcholinesterase Inhibition

Acetylcholinesterase inhibition was assayed using an UV-visible spectrophotometer at 412 nm. Assay buffer was NaCl (100 mM), sodium phosphate (100 mM), pH 7.3. Enzyme stock solutions were prepared with the buffer in the following concentrations: 100 U/mL, and 3 U/mL keeping at 0°C. Then appropriate dilutions of the AChE (1:30) solutions were carried out. Stock solutions of the nanoparticles were prepared in acetonitrile (10, 20 and 30 µg). After, in a cuvette containing acetonitrile (50 µL), assay buffer (830 µL), 5,5′-dithio-bis-(2-nitrobenzoic acid) (DTNB), (50 µL), nanoparticle solution (10 µL) and enzyme solution (10 µL) were added and incubated for 15 min at room temperature. After mixing and bringing the absorbance to zero, substrate (acetylthiocholine; at 0.03 to 0.16 mM) was added to initiate reaction. Assays were carried out at room temperature over a 1 min period, taking readings every 5 minutes [28].

Preparation of in-vitro Glycated Albumin (BSA)

In this work bovine serum albumin (BSA) was used due to it is widely used as a model protein for exogenous and endogenous ligand binding. Briefly, BSA (10 mg/mL) was incubated with glucose (0.5 M; 0.1 M PBS; pH7.4) containing sodium azide (NaN3; 0.02 %) under sterile conditions at 37 °C for 30 days. The blank was test only with BSA . The solution was dialyzed with a one-time exchange of PBS 24 h after. The formation of advanced glycation end products (AGEs) was confirmed and evaluated by fluorescent in glycated albumin samples and of the positive control at excitation and emission wavelengths of 370 and 440 nm (Perkin Elmer luminescence spectrometer LS50B, USA). The evaluation of protein aggregation of the β amyloid structure was measured in agreement with the method of Bouma [29].

Determination of Protein Aggregation

Several laboratory methods with variable sensitivity are employed for detection of protein aggregation among them are ThT, Congo red, turbidimetric aggregation, and dynamic light scattering and analysis. The mode of ThT binding to fibrils is binding to the surface ridges of the b-sheets, interacting particularly with hydrophobic residues across 4 b-strands via electrostatic interactions with the positive charge on ThT. In consequence mode led to a high fluorescent yield [30]. Congo red, one of the most used amyloid-specific dye, Congo red, binding to most amyloids results in a bathochromic shift, birefringence under polarized light, dichroism, and fluorescence [31], involves a cooperative process entailing the formation of a complex with 1:1 stoichiometry. This provides a molecular basis to explain the bathochromic shift in the maximal absorbance wavelength when Congo red is bound to amyloids. Turbidimetric study of heat-induced protein aggregation whit a variety in charge of amino acid side chains leading an alteration of firefly luciferase surface hydrophobicity may control the extent of heat-induced aggregation [32]. Dynamic light scattering can be applied to enabling simultaneous measurement of non-fibrillar precursors and elongating fibrils. More generally, a tool is presented for the investigation of amyloid forming peptides, like polyQ and Aβ, the amyloid inducing peptide in Alzheimer's disease [33]. Based on the above, we

chose these methods to carry out this study.

Turbidimetric Aggregation Analysis

Aβ aggregation was measurement by turbidimetric analysis [34] in the solution of BSA and BSA incubated with ribose (1 mL), BSA-glucose+ CeO2 NPs (2 mg/mL), BSA-glucose To, and BSA-glucose + To/CeO2 NPs(2 mg/mL), at 30 days of incubation at 37°C. The absorbance intensity of control and sugar incubated samples were measured at 450 nm on a Shimadzu UV spectrophotometer UV-1800.

Dynamic Light Scattering and Fluorescence Studies

The size and morphology of the nanoparticles, the growth of macromolecular assemblies through aggregation partway were analyzed by dynamic light scattering (DLS) using a Zetasizer Nano ZSP (Malvern Instruments, Malvern UK). Particle size distribution was determined in a dispersion of BSA incubated with glucose, BSA-glucose+ CeO2 NPs, BSA-glucose + To, and BSA-glucose + To/CeO2 NPs at 30 days of incubation at 37°C, where is determined the protein aggregation given for the intensity fluorescence, size distribution, zeta potential and polydispersity index.

Thermal Aggregation

Sample of BSA-glucose (10 mg each) were incubated along or with the nanoparticles (2 mg/mL) at 60 °C. An aliquot at 3 and 6 h was collected for analyzing structural modification and aggregation then fluorescence was determined at an emission of 440 nm with an excitation wavelength of 355 nm.

Determination of Amyloid β-Aggregation by Thioflavin T (Th.T)

For evaluation of amyloid cross β structure another Thioflavin T marker for β aggregation was used. Glycated BSA samples and positive control (100 µL) were incubated with 32 µM Th. T for 1 h. at 25°C. The Fluorescence was determined at an excitation and emission wavelengths of 435 and 485 nm respectively with correction for background signals without Th. T. The results were expressed as % inhibition, calculated by the formula:

$$\%inhibition = \frac{F0 - F1}{F0} \times 100 \qquad (3)$$

Where F0 is the florescence of the positive control

F1 is the florescence of the glycated albumin samples incubated with nanoparticles.

Binding of Congo Red

Amyloid cross β-structure, a common marker for protein aggregation was measured by using a Congo red test. For this purpose, the glycated BSA samples (50 µL) and positive control were incubated with 50 µL Congo red (100 µM in 10% (v/v) ethanol/PBS) for 20 min at room temperature. The absorbance was measured at 530 nm and recorded for the Congo red background as well as for Congo red incubated samples. The results were expressed as % inhibition according to equation (4):

$$\%inhibition = \frac{A0 - A1}{A0} \times 100 \qquad (4)$$

Where Ao is the absorbance at 530 nm of positive control

A1 is the absorbance at 530 nm of the glycated albumin samples incubated with nanoparticles.

Cytotoxicity of To/CeO2-NPs

Cytotoxicity of GH/CeO2-NPs was evaluated against normal RAW 264.7 macrophage cells obtained from Sigma, St Louis, MO, USA, using 3-(4,5-dimethylthiazol-2-yl)-2,5- diphenyltetrazolium bromide (MTT) assay. Cells (5 × 104 cell/well) were seeded in Dulbecco's modified eagle's medium (DMEM; Gibco) containing 10% fetal bovine serum, 100 µg/mL strepto-

mycin, and 100 U/mL penicillin in a 96 well plate for 24 h incubation at 37 °C in 5% CO2 to reach a cell density of 80% confluence and treated with nanoparticles 0, 18.7, 37.5, 75, 150, 300 and 400 µg/mL. The proposed concentrations were chosen based on previous research performed with CeO2 NPs [44]. Untreated cells and 5% DMSO-treated cells were assayed as negative and solvent control, respectively. After 24 h incubation, 20 µL MTT dye (5 mg/mL) was pipetted in all wells, including wells with untreated cells, and incubated for 4 h. The medium was aspirated, and 100 µL of DMSO was added to all the wells to dissolve the formazan crystals and measured after an hour at 570 nm using a microplate reader. The percentage of cell viability was calculated from the ratio of the absorbance of treated cells with respect to those untreated.

Statistical Analysis

All values were reported as a mean ± SD. Statistical analysis of data was carried out by analysis of Student's t test employing to compare 2 groups for continuous variables with normal distributions and one-way analysis of variance (ANOVA) was used by for multiple groups, with Tukey's post hoc analysis. *p* values less than 0.05 were considered statistically significant.

Results

Characterization of Cerium Nanoparticles and Li Loaded Nanoparticles

UV/Vis Spectrophotometer

The color of the reaction mixture was pale yellow at the initial point of reaction, which gradually is modified to intense yellow (Figure 1); this color was associated with the excitation of surface plasmon the CeO2 nanoparticles, indicating that Ce(NO3)3 is reduced to Ce02 nanoparticle. The Figure 1 shows CeO2 NPs were stable in water with a transparent appearance, which suggests the formation of nanoparticles. UV-Visible spectrophotometry indicated a characteristic absorption peak at 301nm due to the surface plasmon (Figure 1), this absorption was compared with obtained for Ce(NO3)3. 6H2O of 252.5m 267 and 400 nm which confirms the formation of CeO2 NPs. However, UV–visible spectra showed the peaks at 283 and 323 nm for free To extract. Thus, the UV spectra of To/CeO2 NPs centered at 271nm supported that that To extract was successfully absorbed on the surface of nanoparticles, as shown in Figure 1, which correspond to the spectra of Ce(NO3)3.6H2O,To extract, CeO2 NPs, and combination of To with cerium nanoparticles (To/CeO2 NPs). Peaks represents the formation of cerium oxide nanoparticles confirming the formation of To/CeO2 NPs.

Table 1: Effect of BSA-glucose incubated with To, CeO2 NPs, To/CeO_2 NPs and donepezil on Zeta potential, average diameter, polydispersity index and fluorescence for 30 days

Sample	Zeta potential(mV)	Average diameter(nm)	Polydispersity index	Fluorescence (A.U)
BSA	−8.41	9.2	0.13	8.6
BSA/glucose	−34.6	4255	1.0	74.9
BSA/glucose +CeO_2 NPs	-28.4	2765	0.714	47.2
BSA/glucose +To	-26.5	2432	0.772	41.4
BSA/glucose + To/CeO_2 NPs	-19.5	1765	0.674	34.1
BSA/glucose +Donepezil	-29.1	3012	0.938	61.3

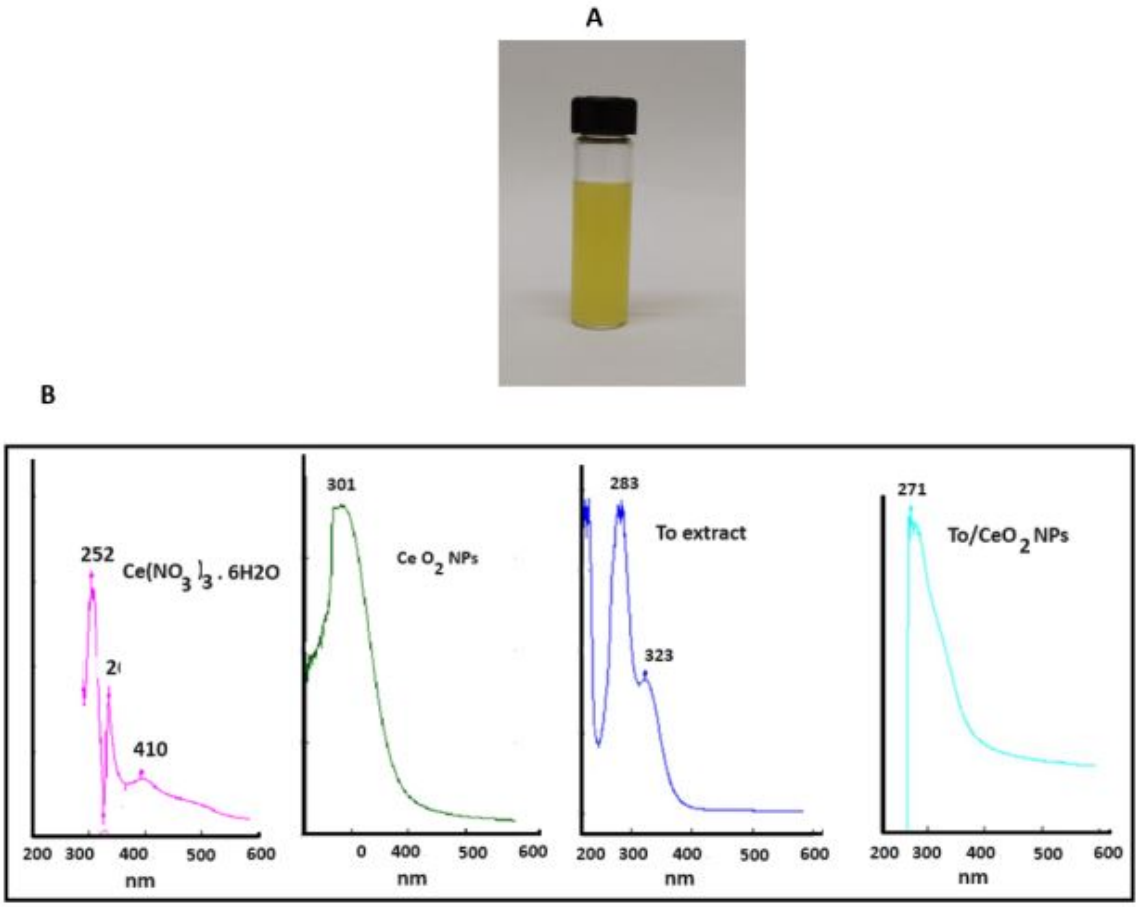

Figure 1(A): Formation of CeO2 NPs (B); UV–visible spectra of Ce(NO3)3.6H2O, CeO2 NPs, To extract and To/CeO2 NPs

Intermolecular Interaction

FT-IR spectroscopy was used to determine the functional groups present on the surface of cerium nanoparticle and also was used to study the possible intermolecular interaction between compounds from lemon peel and nanoparticle, and the infrared spectrogram was displayed in Figure 2. The measurements were recorded over the range from 400 to 4000cm-1. The pink grapefruit spectrum presents the following peaks at 3367, 2921, 2875, 1721, 1612, 1456,1359, 1255, 1177, 1079, 1044 cm.

The peak at 3367 cm-1 corresponds to -OH stretching; the band at 2921 cm−1 associated to CH2 and C-H stretching of aliphatic groups; 1721 cm−1 corresponds to C=O stretching of the carbonyl group; 12cm−1 to aromatic C=C stretching vibration; CH2 bond is associated with the stretching vibration at 1456 and 1359 cm-1 assigned at CH3 bending; 1177cm−1 and 1079 cm−1 at –C–O stretch. Among them, absorptions in 1721, 1612, 1456, and 1359 cm−1 are characteristics of flavonoids. However, CeO2NPs, displayed an intense and broad peak at 3367cm−1, associated with the stretching vibration of O–H corresponds to the bending vibration of water absorbed. Also, bands at 1612 cm−1 and 1456 cm−1 corresponds to H–O–H deformational vibrations; The characteristic peak at 1062 cm−1 corresponds to the C–O antisymmetric stretch, thus the band at 1498 cm−1 is attributed to the symmetric stretching vibration of –O–C–O groups in the formation of CeO2 NPs. Moreover, in To/CeO2 NPs spectrum bands at1721, 1612, 1456, 1255, 1117. 1079 and 1044 cm−1 were abolishment indicating that the corresponding groups directly interacted with Ce NPs staying in the surface of CeO_2 NPs. New peaks appeared in 1750, 1563, 1463, 1367 1311 and 1085 cm−1, associated to C-C and CH stretching bonds. FTIR spectrum of To also indicated that the bands were shifted in the different way that the bands in the spectrum of CeO2 NPs, which could confirm the formation of a layer over cerium oxide core. Thus, it can be inferred that OH groups of flavonoids contents in the extract are involved in binding with cerium oxide nanoparticles.

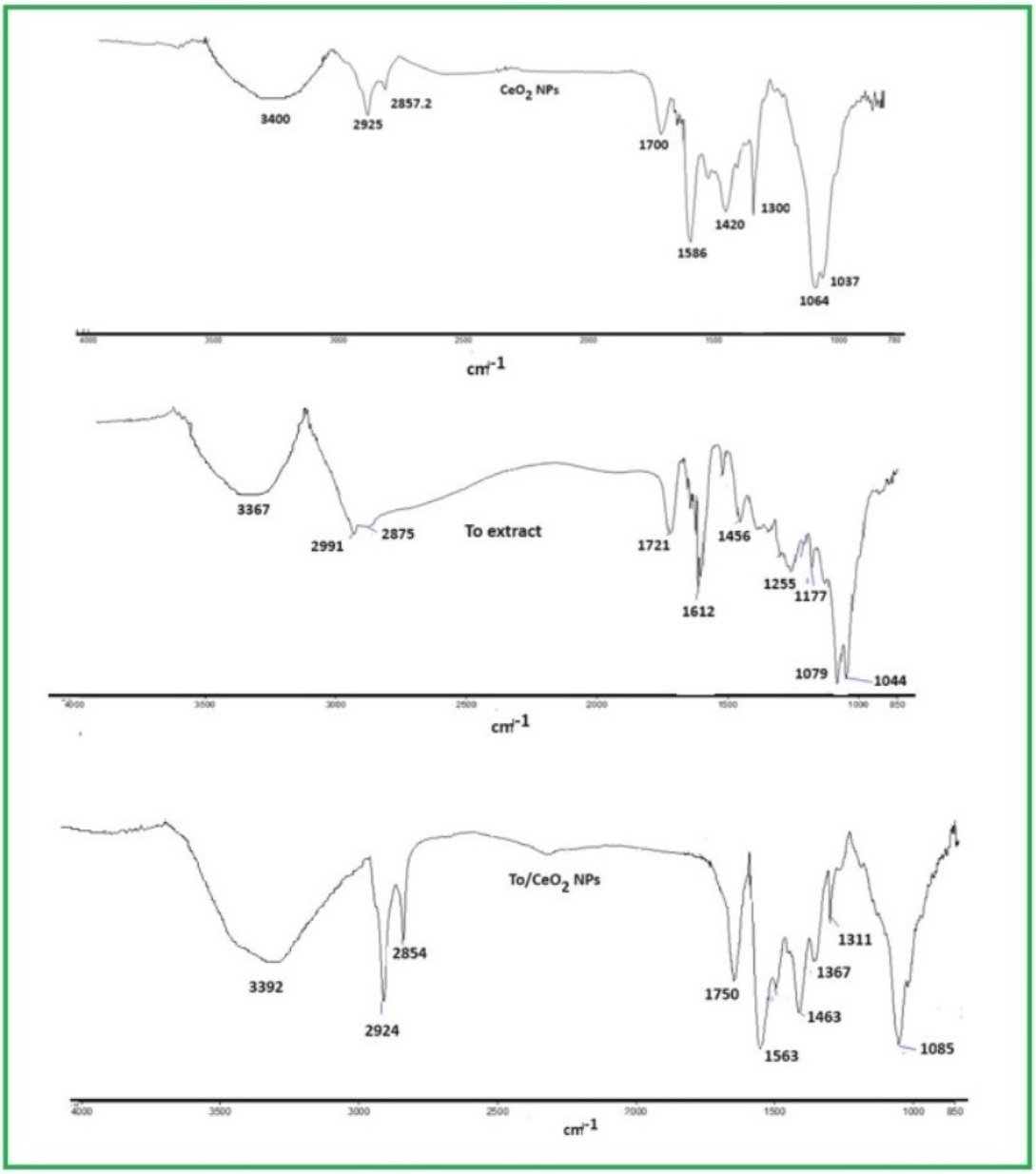

Figure 2: FT-IR spectra of (A) CeO2 NPs; (B) To extract, (C) To/CeO2 NPs

Particle Size Distribution

Yellow elemental cerium was formed by reducing bulk cerium to its nanoform. The average particle size, polydispersity index (PDI), and zeta potential of the cerium nanoparticle and To/CeO2 NPs nanoparticles were measured using dynamic light scattering (DLS). The results revealed formation of cerium nanoparticles in a size range 70.2 < D /nm <-156.5 with an average diameter of 134.6 nm (Figure 3A), a zeta potential of -22.3 mV, and the polydispersity index was found to be 0.240. The Figure 3B shows the analysis of colloidal dispersion of To/CeO2 NPs indicating that synthesized particles had an average size of 199 nm and a zeta potential of -22.6 mV. Polydispersity index was found of 0.460 for extract loaded conjugated nanoparticles demonstrating homogenous size population of nanoparticles in the aqueous medium. The DLS results were also in agreement with TEM date. Nanoceria showed good stability in water in neutral pH that could be attributed to the negative value of zeta potential. The characterization of the To/CeO2 NPs demonstrated the extract encapsulation with high efficiency in spherical shape with smooth surface and in nano size range.

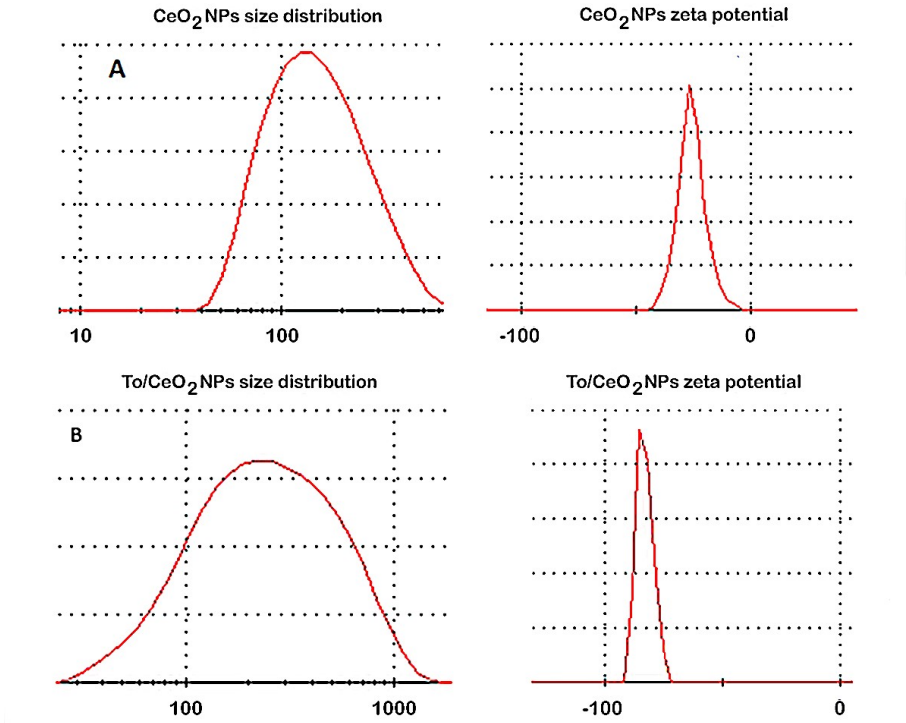

Figure 3: Size distribution and Zeta potential of CeO2 NPs (A); Size distribution and Zeta potential of To/CeO2 NPs (B)

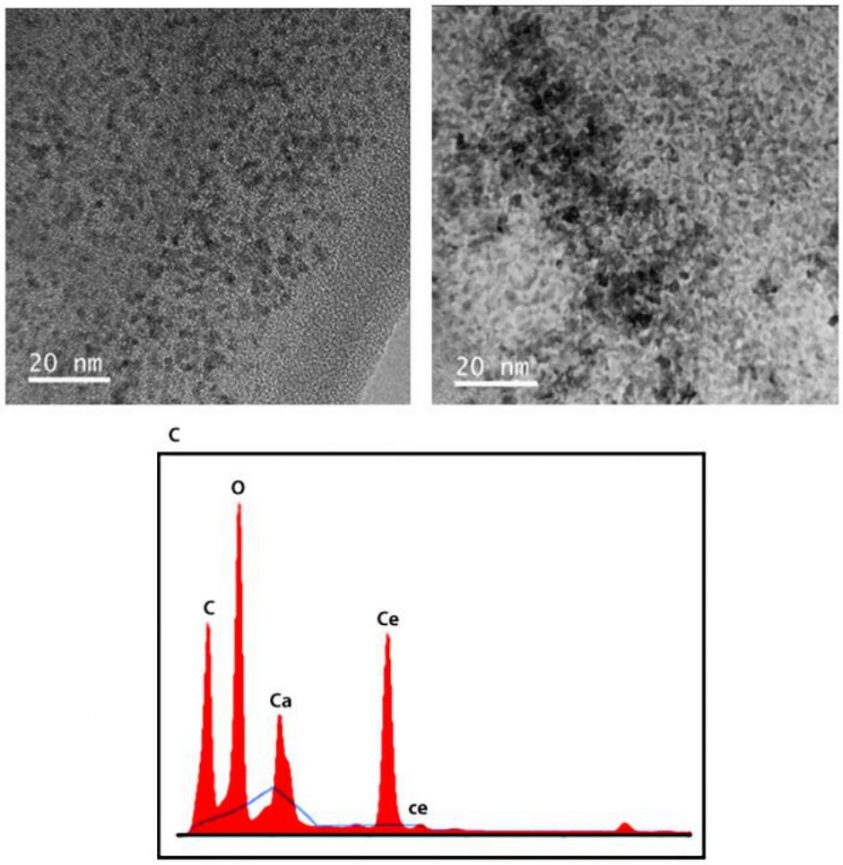

Figure 4: Images of synthesized nanoparticles: (A) CeO2 NPS (50 nm); (B) To/CeO2 NPs (50 nm); (C) Xray Diffraction analysis of To/CeO2 NPs

Transmission Electron Microscopy, Scanning Electron Microscopy

The high-resolution TEM image of CeO2 NPs indicate that have a spherical shape and are moderately agglomerated (Figure 4A). On studying the TEM images of To/CeO2NPs at various magnifications the following characteristics were observed: The To/CeO2NPs was spherical in nature having size ranging between 60-200 nm (Figure 4B). The figures show certain aggregates which are likely to increase the stability of the nanoparticles suspensions. The smaller aggregates in the combines to form larger aggregates. The growth of smaller aggregates tends to form uniform size of regular spherical shape. TEM image revealed a significant difference in chemical composition between the cerium nanoparticles untreated and treated with the treated extract.

X-Ray Diffraction (XRD) Analysis of To/cerium Nanoparticles

Figure 4C represents the analysis of X-Ray diffraction of crystal structure of To/CeO2 NPs with characteristic peaks based on their elemental composition. The diffractogram presented different peaks of elements, including c, O2, Ca together with cerium were also detected. The elemental analysis indicates a peak of cerium around 14.94 % of mass confirming transition from bulk form to nano form.

The pure crystalline phase of To/CeO2 NPs was confirmed by sharpness of the peaks. The identified main elements were carbon and oxygen with 39.99%, 29.42%, (w/w) respectively, while Ca appears with 13.61%. In XRD patterns of the To/CeO2 NPs all the intense and sharp reflection peaks can be indexed to the nanoparticles structure.

Encapsulation Efficiency (EE, %) and Loading Capacity (LC, %) of To in CeO2 NPs

The percentage of the To extract entrapped in CeO2 NPs is known as encapsulation efficiency and is related to the ratio between cerium/To extract, which varying with the solubility of the extract in the matrix material. In this work, the EE was found between 83.4% (1:0.5), 65.7% (1:0.75) and 50.2% (1:1), (Figure 5A). The highest efficiency was obtained at cerium/extract ratio of 1:0.5. The efficiency decreases as the weight ratio between cerium/extract is reduced, due to that the saturation increases, and the excess To extract cannot be adsorbed by CeO2 NPs. Consequently, extract will be easily released during the centrifugation process. LC is the amount of the pink grapefruit peel extract encapsulated per unit weight of the cerium nanoparticles and is significantly affected by molecular weight of the compound contained in the extract encapsulated which led to lower Loading capacity. The loading capacity of the CeO2 NPs ranged from 75.4% (1:0.5), 23.8% (1:0.75) and 18.8 (1:1), (Figure 5B). Nanoparticles were fabricated as nanocarriers for To encapsulation to enhance stability, controlled release, and biological activity. The in vitro drug release studies revealed that To encapsulated in CeO_2 NPs showed a controlled drug release demonstrated that To/CeO2 NPs have an excellent delivery ability.

Phytochemical Analysis

The yield of extraction performed by Ultrasound-assisted extraction was 20.1%. The total flavonoids content in pink grapefruit peel measured by Folin–Ciocalteu method was of 15.7 mg QE/DW consistent with the data reported [35].

To Extract and To/CeO2NPs Inhibited AChE Activity

To find new anti-Alzheimer's activity, we designed and synthesized To/CeO2NPs as cholinesterase inhibitor based on flavonoids content in To extract as the lead compounds. CeO_2NPs, To and To/CeO_2NPs on AChE effect was carried out according to reported by bibliography [28]. The observed results for the AChE inhibitory activity are shown in Fig 5B. At dose of 10, 20 and 30 µg each displayed dose-dependent inhibition on AChE. The finding proves that To/CeO_2NPs at concentration of 20 and 30 µg exhibited moderate AChE inhibitory activities by 59% and 75.1% respectively compared with donepezil used as the positive control about 65.8% and 89% respectively (Figure 5B).

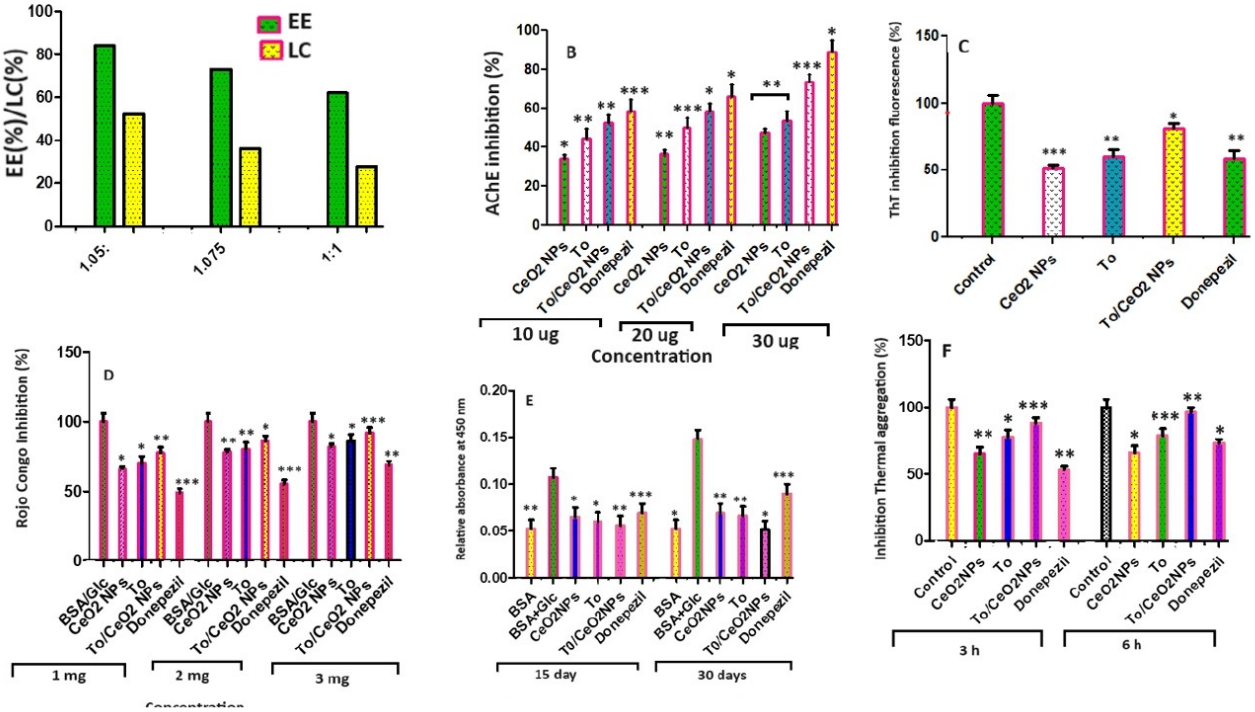

Figure 5: Determination of encapsulation efficiency and Loading capacity obtained at ratio of 1:0.5, 1.075, and1:1 of cerium/Li (A) ; AChE inhibitory activity from CeO2NPs, To and ToCeO2NPs (B); Fibrillation results in ThT test assay at Ex- 440 nm, Em-490 nm generated by CeO2NPs, To and ToCeO2NPs and donepezil in glucose incubated BSA (C); The effect of nanoparticles in vitro formation of amyloid-β products—Congo red dye in BSA-ribose glycation at 490 nm(D); Aβ Aggregation measurement at 15 days and 30 days BSA/glucose incubation by turbidimetric analysis at 450 nm (E);); Aβ Aggregation measurement at 3 and 6 h in BSA/glucose incubation by thermal assay (F); figure are means ±SD; Asterisks (*) indicate significant statistical differences between treated and untreated control °p<0.05; **or°° p<0.01; ***p<0.001

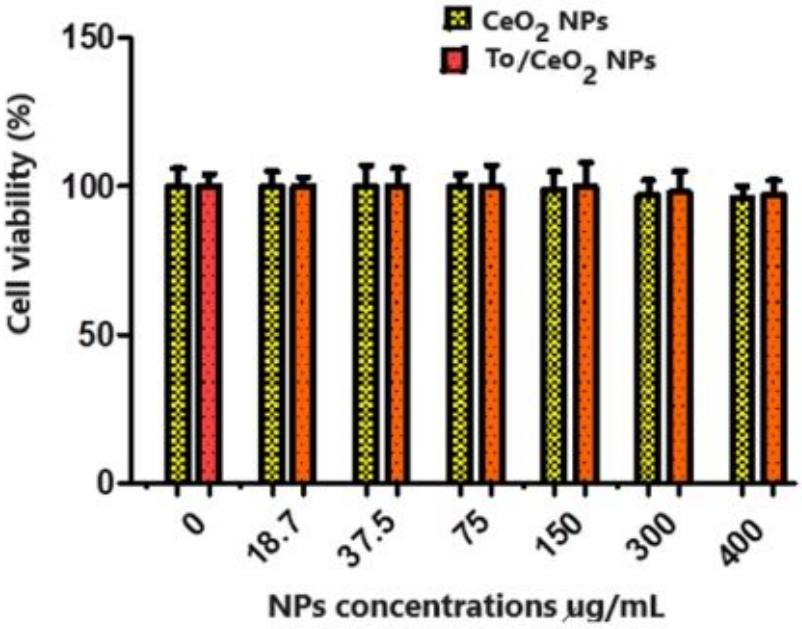

Figure 6: Cells Viability measurements of RAW 264.7cells exposed to Se@BSA NPs and EM/Se@BSA NPs at 0, 18.7, 37.5, 75, 150, 300 and 400 µg/mL. Data are expressed as the mean ± SD

Evaluation of Antiaggregatory Activity

Fluorescence Intensity Studies of Glucose -BSA with Nanoparticles

Altogether, this first use of fluorescence self-quenching for monitoring amorphous aggregation suggests that it could enable the analysis of a molecule's early aggregation phase, The fluorescent AGE formation was evaluated in BSA–glucose. This system was used as a glycation model and monitored throughout 4 weeks of incubation. In this experiment was observed an important ($p< 0.05$) increment in fluorescent intensity in BSA incubated with glucose. The finding indicated that the fluorescent AGE formation was increased by 8.69-fold. Glucose -modified BSA showed higher emission fluorescence intensity 74.8 A.U (arbitrary unit) than native BSA (8.6 A.U) while fluorescence intensity decreased with addition of To, CeO2 NPs, and To/CeO2 NPs in 41.4 A.U, 47.2 A.U and 34.1 A.U. respectively (Table 1).

Dynamic Light Scattering (DLS)

A DLS-based method was developed for the in-process monitoring protein refolding and aggregation reducing process variability and ensures product quality. Aggregation, surface hydrophobicity, and conformational change of a macromolecule can be determined used Zeta potential measurement. Values of Zeta potential of native BSA was found of −8.41mV while glycated BSA showed a value at −34.6mV (Table 1). However, glycated BSA in the presence of CeO2 NPs, To and To/CeO2 NPs exhibited a s reduction in zeta potential values, lower than the donepezil. The increment incubation time in the samples produces light scattering high this mean of hydrodynamic sizer of the molecules in dispersion get bigger indicates that aggregation is produced. Table 1 show that the increment of diameter is less important for nanoparticles than highly glycated albumin. Findings indicated that nanoparticles had stronger inhibition effect on aggregates formation from BSA–glucose model. In addition, the polydispersity indexes indicate the homogenous of the BSA in dispersion (Table 1) with a mono-disperse sample, a PDI of 0.1 or lower is ideal instead a PDI bigger than 0.1 indicates more species are present in the system [36]. Z-average particle sizes of less than 4255 nm for the CeO2 NPs, To and to/CeO2 NPs concentrations and PDI of less than 0.1, indicating that the nanoparticles were near to be mono-disperse.

Thioflavin T (ThT) Fluorescence Spectroscopy

Actually, has been develop fluorescent probes that detect amyloids with different compositions, structures, and sizes in vitro, ex vivo, or in vivo. Thioflavin-T, displays an increase in fluorescence in the presence of large aggregates, and is typically used to assess protein aggregation. Thioflavin T fluorescence experiment in glycated BSA treated with To extract and To/CeO2 NPs was performed to measure the development of aggregated structures. Native BSA show little fluorescence on binding with ThT, as well as glycated BSA and ThT also show notable increment in fluorescence evidencing the formation of aggregated structures according with the previous works. As shown in Figure 5C, a decrement of glycated BSA fluorescence intensity with To extract, CeO2 NPs and To/CeO2 NPs was observed (53%, 49.3% and 75.8% respectively). ThT fluorescence displayed a downward trend, implying towards the protective effect attributed to extract and nanoparticles as well as donepezil used as positive control. In consequence, nanoparticles have ability of avoiding the development of aggregates in glycated BSA. Besides, To/CeO2 NPs was revealed to show more anti aggregation effect that other treatments.

Congo red Assay (CR)

Congo red amyloid specific dye binds mainly to β-sheet conformation of amyloid fibrils. Protein solutions containing amyloid fibrils shifted the spectral properties of Congo red and exhibited a considerable increase in absorption [37]. Congo red, an assay carried out to supporter the prime feature of protein aggregates (formation of β-sheet structures) was performed to complement the results found in ThT fluorescence assay regarding the production of BSA aggregates on sugar incubation. Congo red displayed an absorbance at around 490 nm while on binding with β-sheet structure of amyloid fibrils, absorbance shows a shift from 490 to 540 nm [38]. This research demonstrated that To extract and To/CeO2NPs, inhibit fibril formation in glycated BSA that donepezil which was used as the positive control (Figure 5D). Results indicated that To/CeO2 NPs, is a potent anti-aggregation agent compared with To extract and donepezil. This result agrees with thioflavin T observations.

Turbidity and Thermally Assays

The robustness of a combined DLS system with turbidity and thermally assays for protein thermal stability evaluations has

been documented by the current study. In order to validate the results founding b in UV. Congo red and Thioflavin T assays on the generation of BSA aggregates, turbidity assay was performed at 450 nm. The degree of aggregation of BSA in the absence and presence of glucose was monitored for turbidity determinations. An increment in turbidity was observed after day 22, achieving a maximum around day 30, suggesting the formation of aggregates. In this study was observed that native protein displayer a negligible change in absorbance demonstrating the absence of aggregates implying that BSA is found natural conformation. Figure 5E shown the effect of CeO2 NPs, To extract and To/CeO2 NPs, on the absorbance of glucose incubated BSA at 450 nm. It is observed that after of day 30 the samples turbidity for To extract, CeO2 NPs, and To/CeO2 NPs, showed an effect anti-aggregative. These effect on aggregation proteins was more prominent for To/CeO2 NPs that in the other treatment. Findings indicate that nanoparticles prevent aggregate formation and hindered their formation. Similarly, the thermally treated samples observed the inhibition in B-amyloid aggregates at 3 and 6 h incubation resulting inhibition of B-amyloid aggregates (Figure 5F). At 6 h the B-amyloid aggregates reduced to 87% by To/CeO2 NPs, 57% by CeO2 NPs and 78% by To extract. Thus, glucose treated BSA presented more aggregation than native BSA indicating that nanoparticles inhibited the B-amyloid aggregate formation in the glycation development as well as thermal aggregation.

Cell Viability Assay of Nanoparticles in RAW 264.7 Cells

In addition, to evaluate CeO2 NPs and To/CeO2 NPs safest concentrations on RAW 264.7 macrophages, the nanoparticles were screened using MTT assay. As shown on Fig. 6C, thought this experiment, determined by MTS assays there were not markedly differences between non-pretreated cells and pretreated cells. After 24 hours of incubation, the level of confluence remained very similar. Results indicated that exposure to CeO2 NPs and To/CeO2 NPs, at concentrations of 300 and 400 µg/mL does not produce any substantial negative effect on cell growth. The finding indicated that nanoparticles do not affect cell viability with increasing concentrations of CeO2 NPs and To/CeO2 NPs possibly to avoid accumulation inside the cells, consequently causing decreased cell death and cellular stress.

Discussion

C. paradisi peel extract was conjugated on the surface of CeO2 NPs and characterized using different spectroscopic techniques. This study presents the synthesis of To/CeO2 NPs which highly exhibited stability, nano-size, amorphous nature, and spherical shape. The intensity of the peaks in XRD analysis indicated that the To/CeO2 NPs was in pure crystalline phase. This research provides new insight into the use of nanoparticles in medicine containing cerium and phytocompounds against protein aggregation in vitro. Based on previous studies CeO2 NPs have potent antioxidant and redox properties [39] and the obtained results indicated that they could be promising nanoparticle for therapy of diseases in where oxidative stress plays a critical role such as neurological disorders [40]. Thus, CeO2 NPs because their powerful free radical scavenging ability were used as carrier to load bioactive from lemon peel for the treatment of AD. The compounds of natural source are related with to beverages and common foodstuff use for human consumption. However, these compounds had not a favorable development as drugs due to poor bioavailability and water solubility.

The flavonoids possess a poor absorption and bioavailability profile in vitro test indicate that cannot recommended as drug candidates [41]. Numerous pharmacological investigations have found that flavonoids have important therapeutic activities on neurodegenerative diseases through of a mechanism multifactorial, which includes antioxidant effect [42]. Free radical (ROS) are a contributing factor in the progress of neurodegenerative diseases as AD generating reduction of mitochondrial function, decrease antioxidant system and modified metal homeostasis, in consequence they produce an alteration neurotransmission in neurons and in the synaptic activity leading to cognitive dysfunction [43]. Glycation is able to cause protein crosslinking and aggregation, leading to β-amyloid fibrillation. Accumulation of β-amyloid fibrillation adducts promoted the pathological progression in neurodegenerative disorders [44]. Based on this evidence have investigate for the first time the combination of lemon peel extract with cerium nanoparticles in promising levels of neuroprotection and their hypothesized mechanism of action focuses on vitro assays, we have caried out a series of techniques and test to evaluate the structural changes related to in vitro aggregation on incubation with glucose.

To peel extract was obtained by Ultrasonic-assisted extraction due to reduction of extraction time owing can produced cell wall disruption. Consequently, sonication of lemon peel was used for us as a pre-treatment technique to improve the bioaccessibility of the total polyphenolic content and other bioactive. Also, we studied the effect of To/ CeO2 NPs in the established Ellman's colorimetric assay for evaluating the expression of AChE enzyme. Findings indicate that To/ CeO2 NPs significantly show inhibition of this enzyme. In addition, the observed results were inferior to those of donepezil, at the same concentration, suggesting that the mechanism (s) of action implicate in the activity of the nanoparticle could be in part similar to the mechanism of donepezil and other type of mechanisms which could contribute to ameliorate the disease. Donepezil is a representative AChE inhibitor that improves damaged nerve endings to communicate with other nerve cells. Which was used in this study as positive control? Results indicated a better inhibitory activity with donepezil, than other samples. Inhibition screening against acetylcholinesterase (AChE) indicated that all synthesized compounds possessed potent AChE effects. The variation in the level AChE may be a potential in vivo diagnostic marker for AD, especially when used in neurological disorders associated with dysregulation of AChE activity.

The aggregation of protein accumulates in tissues mainly by thermal denaturation, metabolic reaction and interaction with drugs, are found in neurodegenerative and metabolic disorders. This work investigates the effect of nanoparticles in glucose-induced aggregation on BSA structure. Finding for thioflavin T showed that for BSA, the level of amyloid structure was inhibited by To, and nanoparticles. A strong protection of BSA was observed for To/CeO2 NPs. A similar trend of results was showed with the Congo red test. The fluorescence intensities of glycated BSA were about 8.69-fold than the native BSA results in amyloid aggregation, which is closely associated to AD. The addition of glucose produces to an increment in the β-sheet conformation in BSA. In addition, high plasma amyloid-β concentrations are related with an increase of developing AD disease. However, inhibition of fluorescence intensity in incubated sample with nanoparticles compared to native BSA clearly demonstrated the inhibition of aggregates formation. In the case of Aβ1–42, in the presence of nanoparticles in experimental incubation conditions resulted in a significantly decrease of fluorescence intensity while in Aβ1–42 untreated displayed high fluorescence intensities, indicated an important conformational modified of peptide. Results suggested that the decrease of fluorescence intensities may be to the quenching of amino acid residues by nanoparticles. This interaction produces a reducing effect of nanoparticles on Aβ1–42 than donepezil and possibly has the ability to discontinue in β-sheets the fibril-stabilizing bonds. The change in the amino acids inside amyloidogenic places plays an important role in reduction amyloid formation [45]. In this investigation, we determined that To/CeO2 NPs decrease of amyloid AB1-42 accumulation in consequence the effect therapeutics of To/CeO2 NPs on amyloid aggregation possibly can interact with intermolecular β-sheet region in Aβ42 aggregates through hydrophobic forces, hydrogen bonds, and Vander Waals forces inhibiting the protein aggregation [46] and the chemical structure of flavonoids with their carbonyl groups could combine with lysine residues and damage the self-assembly process of nucleation and elongation of fibril formation avoiding protein aggregation. Findings of this investigation are consistent to those of Zeta potential, polydispersity index and hydrodynamic diameter. Usually, modified proteins by glycoxidation reaction produce alterations in their electrophoretic mobility, isoelectric point, and surface hydrophobicity. However, glycation produce partial unfolding of proteins, modifying the electrophoretic properties. In this work To/ CeO2 NPs prevents the loss of secondary structural elements in the glycation due the ability of extract and CeO2 NPs to scavenge free radicals and their synergic effect generating a potent reductor effects on protein glycation attributed to the protection of structural modifications and surface hydrophobicity in protein.

In our work, protein aggregation was measured using the amyloid-β-specific pigments, Congo red and thioflavin T. Finding of thioflavin T show ed that for BSA, the level of amyloid structure was inhibited by To, and nanoparticles and a strong protection of BSA was observed for ToCeO2 NPs. A similar trend of results was showed with the Congo red test.

The thermal glycation and the turbidity observed in BSA in the presence of sugar result are the aggregation of β-amyloid structure which was reversed with To/CeO2 NPs treatment suggested inhibition of larger aggregates formed. These observed findings indicate that nanoparticles effectively inhibiting glycation--induced aggregation.

Natural compounds that exhibit anti-amyloid and anti-aggre-

gation effects have distinct advantages over other synthetic compounds: they are often naturally consumed as part of a healthy diet wherein they offer general nutraceutical benefits such as reduced risk for AD [46]. CeO_2 NPs and polyphenols content in To extract are a rich source for a variety of different structural backbones that can be utilized in rational drug design efforts to find multifunctional anti-amyloid aggregation agents. Thus, the use of To/CeO2 NPs for neurological applications is very promising, such as creating new neuroprotective drugs for the treatment and prevention of neurodegenerative diseases of the brain based on the composition of nanoparticles. Therefore, the presented research in this brief report was to show the cerium and To extract effect.

In the current study, we observed that To/CeO2 NPs synthesized by sol-gel method were no toxic to RAW 264.7 murine macrophage line after 24 h exposure, this effects occurred mostly at a high concentration (400 µg/mL). Due to the low toxicity of nanoparticles, it can be noted in the case of potential use of To/CeO2 NPs for biomedical applications such as AD treatment.

These promising activities of To peel can be attributed to flavonoids components. According to flavonoids reported from previous studies, Hesperidin, a flavanone glycoside, is able to cross the blood–brain barrier and has high antioxidant effects and also inhibited amorphous aggregation of the protein of egg-white lysozyme [45]. Naringin ameliorate platelet aggregation and suppressed the excessive release of PF4 and P-selectin in hyperlipidemic rabbits [47]. Naringenin inhibit the protein aggregation produced in mammalian cells by EGFP-polyQ97 [48]. In other study demonstrated that Naringin and Naringenin decreased the presence of fibrillar aggregates in modified HSA by ribose and glyoxal [49]. Kaempferol interacted with small aggregates of Ab42, but not with the monomer of amyloid β-protein (Ab42) suppressing the elongation and the nucleation phase [50]. Also, Kaempferol possess a significant binding and a considerable residual energy contribution with mutant SOD1 inhibiting the β-sheet content increasing the mutant conformational flexibility and stability [51]. Diosmin shown antiplatelet effects through impedance aggregometry [52]. Rutin exerted diverse effects simultaneously on tau protein in vitro such as reduces tau oligomer and tau aggregation induced cytotoxicity [53]. Sodium rutin administration contributes to microglial recruitment to the plaques and ameliorates αβ-phagocytosis [54]. These flavonoids contained into peel could protect against glycation induced by free radicals decreasing the self-oxidation of sugars and acting as divalent metal ion chelators [55]. Among flavonoids of *C. Lemon* limonin, neohesperidin, hesperidin, naringin, isonaringin and neoeriocitrin significantly possesses acetylcholinesterase inhibition [56].

Conclusion

The cerium oxide nanoparticles were synthesized effectively through a Sol-gel synthesis route using ammonia as a reducer. Synthesized nanoparticles highly present stability, nano--size, amorphous nature, spherical shape and are in pure crystalline phase. The present study provides evidence that the nanoparticles no exerted cytotoxic effects on RAW 264.7 macrophages at concentration of 400 µg/mL. The induction of b-amyloid structure in BSA glucose system was suppressed in the presence of CeO2 NPs, To extract, To/CeO2 NPs and donepezil. To/CeO2NPs was observed to be more potent in impeding the development of aggregates in BSA-glucose system than other samples. The combined To and CeO2 nanoparticles efficiently improvement aggregation proteins to prevent or delay formation of fibrillar species or aggregated of amyloid proteins, characteristics of amyloid fibril formation in AD disease. Anti-aggregating abilities could be through anti-amyloidogenic, and anti- AChE effects. These findings showed that nanoparticles have a promising role as drug anti-aggregating against neurodegenerative disorders. However, much more needs to be make, especially in vivo experiments in animals such as rodents, zebrafish and *Drosophila melanogaster* to be transferred to clinical studies.

Declarations

Competing Interest Statement

The authors declare no conflict of interest.

Acknowledgements

This research was conducted by the support of Instituto Politécnico Nacional in 2022-23.

References

1. Alam P, Siddiqi K, Chturvedi SK, khan RH (2017) Protein aggregation: from background to inhibition strategies. Intern. J. Biol.Macromol. 103: 208-19.

2. Amin S, Barnett GV, Pathak JA, Roberts CJ (2014) SarangapaniPS. Protein aggregation, particle formation, characterization & rheology. Curr. Opin. Colloid. Interface. 19: 438-49.

3. Tellone E, Galtieri A, Russo A, Ficarra S (2019) Protective effects of the caffeine against neurodegenerative diseases. Curr.Med.Chem. 25: 5137-51.

4. Thal LJ (1991) Physostigmine in Alzheimer's disease. In: Becker R, Giacobini E.eds. Cholinergic for Alzheimer therapy Boston: Birkhauser. 107-15.

5. Hill E, Goodwill AM, Gorelik A, Szoeke C (2019) Diet and biomarkers of Alzheimer's disease: A systematic review and metanalysis. Neurobiol.Aging. 76: 45-52.

6. Ferreira-Vieira TH, Guimaraes IM, Silva FR, Ribeiro FM (2016) Alzheimer's disease: Targeting the cholinergic system. Neuropharmacol. 14: 01-15.

7. Artus RT, Dean RL, Beer B, Lippa AS (1982) The cholinergic hypothesis of geriatric memory dysfunction. Science. 217: 408–17.

8. Pope C, Karanth S, Liu J (2005) Pharmacology and toxicology of cholinesterase inhibitors: Uses and misuses of a common mechanism of action. Environ. Toxicol.Pharmacol. 19: 433-46.

9. Kihara T, Shimohama S (2004) Alzheimer's disease and acetylcholine receptors. Acta Neurobiol. Exp. 64: 99-105.

10. Miyazawa M, Tougo H, Ishihara M (2001) Inhibition of acetylcholinesterase activity of essential oil from Citrus paradisi. Nat. Prod. Lett. 15: 205-10.

11. Ayokunle O,Ademosun F, Oboh G (2014) Comparison of the inhibition of monoamine oxidase and butyrylcholinesterase activities by infusions from green tea and some citrus peels. Int. J. Alzheimer's Dis. 2014: 586407.

12. Mallick N, Khan RA (2015) Behavioral effects of citrus paradisi in rats. Metabolic Brain Disease, 31: 329-35.

13. Mohebali N, Fazeli SA, Ghafoori H, Farahmand Z, MohammadKhan iE et al. (2018) Effect of flavonoid rich extract of Capparis spinosa on inflammatory involved genes in amyloid beta peptide injected rat model of Alzheimer's disease. Nutr.Neurosci. 21: 143-50.

14. Calderaro A, Patanè GT, Tellone E, Barreca D, Ficarra S et al. (2022) The neuroprotective potentiality of flavonoids on Alzheimer's disease. Int.J.Mol.Sci. 23: 14835.

15. Morris MC, Tangney CC, Wang Y, Sacks FM, Bennett DA et al. (2015) MIND diet associated with reduced incidence of Alzheimer's disease. Alzheimer's Dement. 11: 1007-14.

16. Li J, Sun M, Cui X, Li C (2022) Protective effects of flavonoids against Alzheimer's disease: Pathological hypothesis, potential targets, and structure-activity relationship. Int. J. Mol. Sci. 23: 10020.

17. Nogata Y, Sakamoto K, Shiratsuchi H, Ishii T, Yano M (2006) Flavonoid composition of fruit issues of Citrus Species. Biosci. Biotechnol. Biochem. 70: 178-92.

18. Barreca D, Bisignano C, Ginestra G, Bisignano G, Bellocco E et al. (2013) Polymethoxylated, C- and O-glycosyl flavonoids in tangelo (Citrus reticulata×Citrus paradisi) juice and their influence on antioxidant properties. Food Chemistry. 141: 1481-8.

19. Deng M,Xuchao L, Huang JF, Chi J, Muhammad Z et al. (2022) The flavonoid profiles in the pulp of different pomelo (Citrus grandis L. Osbeck) and grapefruit (Citrus paradisi Mcfad) cultivars and their in vitro bioactivity. Food Chem.X, 5: 100368

20. Ferreira JF, Luthria DL, Sasaki T, Heyerick A (2010) Flavonoids from Artemisia annua L. asantioxidants and their potential synergism with artemisinin against malaria and cancer. Molecules. 15: 3135-70.

21. Reddy AVB,Moniruzzamanm M, Madhavi V, Jaafar J (2020) Recent improvements in the extraction, lean up and quantification of bioactive flavonoids. Stud Nat Prod Chem. 66: 197-223.

22. Maccarone R, Tisi A, Passacantando M, Ciancaglini M.

Ophthalmic Applications of Cerium Oxide Nanoparticles. J. Ocul. Pharmacol.Ther.

23. Naha PC, Hsu JC, Kim J, Shah S, Bouché M et al. (2020) Dextran coated cerium oxide nanoparticles: a computed tomography contrast agent for imaging the gastrointestinal tract and inflammatory bowel disease. ACS Nano.

24. Sadidi H, Hooshmand S, Ahmadabadi A, Javad Hoseini S, Baino F, Vatanpour M et al. (2020) Cerium oxide nanoparticles (nanoceria): hopes in soft tissue engineeringMolecules. 25: 4559.

25. Zhang M,Zhu S, Yang W,Huang Q,Ho C (2021) The biological fate and bio efficacy of citrus flavonoids:bioavailability, biotransformation, and delivery systems. Food Funct. 12: 3307-23.

26. Moussa Z, Hmadeh M, Abiad MG, Dib OH, Patra D (2016) Encapsulation of curcumin in cyclodextrin-metalorganic frameworks: Dissociation of loaded CD-MOFs enhances stability of curcumin. Food Chem. 212: 485-94.

27. Anand V, Ksh V, Kar A, Varghese E, Vasudev S et al. (2023) Encapsulation efficiency and fatty acid analysis of chia seed oil microencapsulated by freeze-drying using combinations of wall material. Food Chem. 430: 136960.

28. Ellman GL, Courtney KD, Andres V, Feather-Stone RM (1961) A new and rapid colorimetric determinationof acetylcholinesterase activity. Biochem. Pharmacol. 7: 88-95.

29. Bouma B, Kroon-Batenburg LM, Wu YP, Brunjes B, Posthuma G et al. (2003) Glycation induces formation of amyloid cross-β structure in albumin. J. Biol. Chem. 278: 41810-9.

30. Groenning M (2010) Binding mode of Thioflavin T and other molecular probes in the context of amyloid fibrils-current status. J. Chem. Biol. 3: 18-124.

31. Espargaró A, Llabrés S, Saupe SJ, Curutchet C, Luque FJ et al. (2020) On the Binding ofCongo Red to Amyloid Fibrils. AngelateChemie International Edition, 59: 8104-7.

32. Gharanlar J, Hosseinkhani S, Sajedi RH, Yaghmaei P (2015) The effect of surface charge Saturation on Heat-induced Aggregation of Firefly Luciferase. Photochem.Photobiol. 91: 115-64.

33. Streets AM, Sourigues Y,Kopito RR,Melki RM, Quake SR (2013) Simultaneous measurement of amyloid fibril formation by dynamic lights catering and fluorescence reveals complex kinetics. PLOS ONE. 8: e54541.

34. Wang SS, Chen P, Hung Y (2006) Effects of p-benzoquinone and melatonin on amyloid fibrillogenesis of then egg-white lysozyme Steven. J. Mol.Catal. B: Enzymatic. 43: 49-57.

35. Singh B, Singh JP,Kaur A, Singh N (2020) Phenolic composition, antioxidant potential and health benefits of citrus peel. Food Res. Intern. 132: 109114.

36. Nobbmann U, Connah M, Fish B, Varley P, Gee C et al. (2007) Dynamic light scattering as a relative tool 622for assessing the molecular integrity and stability of monoclonal antibodies 623. Biotechnol Genet Eng Rev. 24: 117-28.

37. Lieu VH, Wu JW, Wang SS, Wu CH (2007) Inhibition of amyloid fbrillization of hen egg-white lysozymes by rifampicin and p-benzoquinone. Biotechnol Prog 23: 698-706.

38. Semedo MC, Karmali A, Fonseca L (2015) A high throughput colorimetric assay of β-1,3-D-glucans by Congo red dye. J Microbiol Methods. 109: 140-248.

39. Nikitchenko YV, Klochkov V, Kavok NS (2023) CeO2 nanoparticles improve rooxidant/antioxidant balance, life quality and survival of old male rats. Biogerontology. 24: 47-66.

40. Kim J, Hong G, Mazaleuskaya L, Rosario-Berrio Hs, Grosser DN et al. (2021) ACS Appl Mater Interfaces. 13:60852-64.

41. Ross JA, Kasum CM (2002) Dietary flavonoids: bioavailability, metabolic effects, and safety. Annu Rev Nutr. 22: 19-34.

42. Tonnies E, Trushina E (2017) Oxidative stress, synaptic dysfunction, and Alzheimer's disease. Alzheimer'sDisease.57: 1105–21

43. Agnello L, Ciaccio M (2022) Neurodegenerative Diseases: From Molecular Basis to Therapy. Int J Mol Sci. 23: 12854.

44. Martínez-Herrera M, Figueroa-Gerstenmaier S, López-Camacho PY, Millan-Pacheco C, Balderas Altamirano MA et al.

(2022) Multiadducts of c60 modulate amyloid-fibrillation with dual acetylcholinesterase inhibitionand antioxidant properties: in vitro and in silico studies. J Alzheimers Dis. 87: 741-59.

45. Tupe RS, Kemse NG, Khaire AA, Shaikh SA (2017) Attenuation of glycation-induced multiple protein modifications by Indian antidiabetic plant extracts. Pharm Biol. 55: 68-75.

46. Stefani M,Rigacci S (2013) Protein folding and aggregation into amyloid: the interference by natural phenolic compounds. IntJMolSci. 14: 12411–57.

47. Xiao Y, Li LL, Wang YY, Guo JJ, Xu WP, et al. (2014) Naringin administration inhibits platelet aggregation and release by reducing blood cholesterol levels and the cytosolic free calcium concentration in hyperlipidemic rabbits. Exp Ther Med. 8: 968-72.

48. Yamagishi N, Yamamoto Y, Noda C, Hatayama T (2012) Naringenin inhibits the aggregation of expanded polyglutamine tract-containing protein through the induction of endoplasmic reticulum chaperone GRP78. Biol Pharm Bull. 35: 1836-40.

49. Sarmah S, Goswami A, Kumar, Belwal V, Singha Roy A (2022) Mitigation of ribose and glyoxal induced glycation, AGEs formation and aggregation of human serum albumin by citrus fruit phytochemicals naringin and naringenin: An insight into their mechanism of action. Food Res Int. 157: 111358.

50. Hanaki M, Murakami K, Akagi K, Irie K (2016) Structural insights into mechanisms for inhibitingamyloid β42 aggregation by non-catechol-type flavonoids. . Bioorg Med Chem. 24: 304-13.

51. Srinivasan E, Rajasekaran R (2018) Comparative binding of kaempferol and kaempferide on inhibiting the aggregate formation of mutant (G85R) SOD1 protein in familial amyotrophic lateral sclerosis: A quantum chemical and molecular mechanics study. Biofactors. 44: 431-42.

52. Zaragozá C, Monserrat J, Mantecón C, Villaescusa L, Álvarez-Mon MÁ, et al. (2021) Binding and antiplatelet activity of quercetin, rutin, diosmetin, and diosmin flavonoids. BiomedPharmacother.141: 111867.

53. Sun XY, Li LJ, Dong QX, Zhu J, Huang YR, et al. (2021) Rutin prevents taupathology and neuro inflammation in a mouse model of Alzheimer's disease. J Neuroinflammation. 18: 131.

54. Pan RY, Ma J, Kong XX, Wang XF, Li SS, et al. (2019) Sodium rutin ameliorates Alzheimer's disease-like pathology by enhancing microglial amyloid-β clearance. Sci Adv. 5: eaau6328.

55. Silvan JM, Srey C, Ames JM, Castillo MD (2014) Glycation is regulated by isoflavones. Food & Function, 5: 2036-42.

56. Liu C, Hou W, Li S, Tsao R (2020) Extraction and isolation of acetylcholinesterase inhibitors from Citrus limon peel using an in vitro method. J Sep Sci. 43: 1531-43.

57. Rahman MM, Rahaman MS, Islam MR, Rahman F, Mithi FM, Alqahtani T (2021) Role of Phenolic compounds in human disease: Current knowledge and future prospects. Molecules. 27: 233.

58. Shin S, Lee J, Yoon SH, Park D, Hwang JS, Jung E (2022) Anti-glycation activities of methyl gallate in vitro and in human explants. J. Cosmet. Dermatol. 21: 2602-9.